Renewable Energy 180 (2021) 424–437

Contents lists available at ScienceDirect

Renewable Energy

journal homepage: www.elsevier.com/locate/renene

A comparative study between racking systems for photovoltaic power systems

A. Barbón [a], P. Fortuny Ayuso [b], L. Bayón [b, *], C.A. Silva [c]

[a] Department of Electrical Engineering, University of Oviedo, Spain
[b] Department of Mathematics, University of Oviedo, Spain
[c] Center for Innovation, Technology and Policy Research –IN+, Instituto Superior Técnico, University of Lisbon, Portugal

A R T I C L E I N F O

Article history:
Received 30 January 2021
Received in revised form
13 July 2021
Accepted 18 August 2021
Available online 24 August 2021

Keywords:
Photovoltaic power systems
Racking systems with solar tracker
Racking systems without solar tracker
Optimum tilt angle

A B S T R A C T

We present a comparative study of the different racking systems used in photovoltaic power systems, with a new methodology for determining the total energy produced by each one under usual weather conditions (not clear-skies). In systems without solar tracker, the tilt angle is a major factor contributing to the energy production, and its optimization is essential. We study the effect of tilt update frequency (daily, monthly, or constant) on the total irradiation received by a plane surface, and present a method for computing the optimal tilt angle, which we validate using previous studies. This method is easily implemented, accurate, and valid for any location. We compare all the systems with the most energy-productive one, the dual-axis tracker, in two ways: with respect to energy production, and to levelized cost of energy, both in 39 cities around the World. The results provide a new insight on the relative and objective value of trackerless systems, and some remarkable properties arise, which may be relevant in budgetary consideration.

1. Introduction

In 2018, the global primary energy consumption grew by almost twice its 10-year average of 1.5% per year, with renewable energies accounting for the second largest increase [1], which forecasts an important reduction in the dependence on fossil fuels. Solar energy, which is the main source of energy on Earth [2] is the topic of our work, mainly photovoltaic power systems (PVPS), their economic efficiency (see Ref. [3] for a survey), and applications. In 2018, about 103 (GW) of new PVPS was installed [4], and the total global installed capacity of PV energy was around 512 (GW), 1.3 times what it was in 2017 [4]. The economic efficiency is measured using the so-called levelized cost of energy (LCOE), in USD/kWh. Its weighted average in 2018 was 0.085 (USD/kWh), and it is forecast to be between 0.02 and 0.08 (USD/kWh) by 2030, and between 0.014 and 0.05 (USD/kWh) by 2050 [5].

There are nowadays two kinds of racking systems used in PVPS: with, and without solar tracker. Those with solar tracker are classified according to their motion:

(i) With two axes of rotation (dual-axis trackers), which generate the greatest amount of energy. They are adjusted in real time in order to minimize the angle of incidence of the solar rays reaching its surface. Two PV plants for power generation which use this system are: the Ciurbesti Photovoltaic Park (1.0 MW) in Miroslava (Romania) [6], and the plant at Yunnan (9 MW), China [7].
(ii) With a single axis of rotation, which can have different orientations: horizontal North-South (named “single-axis trackers aligned with the North-South axis”), horizontal East-West (named “single-axis trackers aligned with the East-West axis”), or parallel to the Earth's axis (named “Polar axis trackers”). These have also real-time adjustment. In practice, the most used is the North-South aligned. Examples of PV plants using this design are: CSF SEVILLA (39.984 MW) in Sevilla (Spain), and Northern Light (141 MW) in Copiapó (Chile) (both with North-South axis).

In racking systems without solar tracker, the PV modules have a fixed tilt angle for a fixed period of time and are always South-oriented (in the Northern hemisphere). The tilt angle may be adjusted with different frequencies (daily, monthly) or left constant, the latter being by far the most frequent solution.

* Corresponding author.
E-mail address: bayon@uniovi.es (L. Bayón).

https://doi.org/10.1016/j.renene.2021.08.065
0960-1481/

Commercial PV plants for power generation using these systems are: the Mohammed bin Rashid Al Maktoum Solar Park (613 MW) in Saih Al-Dahal (United Arab Emirates) (constant tilt), and Telangana I (10 MW) in Telangana (India) (Seasonal varying tilt angle) [7].

Although dual-axis trackers have the greatest total energy production, they need not be optimal for a specific installation. Other factors to be taken into account are: initial investment cost, required area for the installation, soil conditions, topography …:

(i) *Initial investment cost.* Dual axis tracker systems are more expensive to procure and install: they generally add a premium of 40–50% to the average deployment costs with respect to a system of the same size without solar tracker, and 20 − 25% with respect to a similarly-sized single-axis tracker system [8]. The use and cost of land is not contained as an input parameter.
(ii) *Soil condition.* Solar trackers add torque to the foundations of the system, which may need to be larger and placed deeper, increasing the cost of the civil work. Actually, the installation of trackers may be prevented to all practical purposes if there is no shallow bedrock.
(iii) *Topography.* Solar trackers are only viable in relatively flat locations, so much so that they cannot be installed in places with inclinations greater than 15° [8]. Thus, previous to the installation, ground undulations may need to be leveled to a certain tolerance. This may increase the deployment cost and make them uneconomical [9].
(iv) *Expected lifespan.* Moving parts are one of the main drawbacks in this respect. This makes trackerless systems optimal for very long lived installations, and single-axis trackers better than dual-axis ones [8].
(v) *Operation and maintenance costs.* There is no standardized notion of annual operation and maintenance cost [10]. However, according to Ref. [11], a reasonable expectation for these annual costs of PV systems is around 0.5% and 1% of the initial investment for large and for small systems, respectively.
(vi) *Wind loads.* When the wind speed is greater than 70 km/h [8], systems with solar tracker turn to their safety position. In it, the solar irradiance absorbed by the system is very low compared to the optimal one. Obviously, trackless systems have not this problem.

All the above factors influence the installation of a PV system with or without trackers. In this paper, our analysis will also cover trackless systems whose tilt can be updated at different frequencies, as explained above (daily, monthly …). In order to make an informed assessment prior to deployment, one needs to have a good forecast of the total energy produced by the system, using different tracking methods. This comparison is the aim of this paper.

From the point of view of efficiency (both energetic and budgetary), the installation angles of a racking systems without solar tracker are key. The two main angles are: tilt and surface azimuth. The tilt angle (β) is the angle between the plane of the surface and the horizontal plane. The surface azimuth angle (γ) is the angle between the projection on a horizontal plane of the normal to the tilted surface and the geographical South (East being negative and West positive). The optimum surface azimuth angle for these systems is, usually, in the northern hemisphere, $\gamma_{opt} = 0°$ (In the southern hemisphere, $\gamma_{opt} = 180°$) [12], so that it requires no discussion. For its part, the tilt angle β is a critical parameter, and knowledge of its optimum provides a great economic benefit. Some factors which influence the value of this optimum are, among others: (1) the period during which β is constant, which can vary from minutes to the whole year, (2) the location of the installation: ground, roof, balcony…(3) the latitude of the place, (4) weather conditions, (5) climatic conditions (polluted air, snow fall, dust storms).

Numerous papers study the optimum tilt angle of racking systems without solar tracker with constant tilt, at different sites throughout the World [13,14]. Their models differ in simplicity of use and accuracy. Roughly speaking, these models can be grouped in two categories: those based on the latitude, in which the optimal tilt angle is taken as the latitude plus or minus a specific value obtained via analytic methods (v.gr. regression analysis), and those who try to maximize the total irradiation falling onto the tilted surface. The former are very simple but prone to error, while the latter, generally more accurate, depend strongly (for their accuracy) on the model of solar irradiance they use; furthermore, their utilization is more complex.

Assuming that the installation of one of these systems is South oriented, Jiménez et al. [15] suggest that the optimum tilt angle (constant throughout the year) is $\beta_{opt} = \lambda - 10.38°$ for Barcelona (Spain) (whose latitude is $\lambda = 41.38°$) and $\beta_{opt} = \lambda - 8.77°$ for Jaen (Spain) ($\lambda = 37.77°$). Darhmaoui et al. [16] obtained $\beta_{opt} = \lambda - 2.06°$ for Lyon (France) ($\lambda = 45.76°$). They, and other authors, also present other optimum tilt angles for places around the world [16,17]. The seek for a formula for the optimum tilt angle depending on the latitude is an active area of research. The hemisphere is usually divided into two halves: $\lambda < 45°$ and $\lambda \geq 45°$ [18]. For locations with $\lambda < 45°$, one of the most used formulas appears in Ref. [19]: $\beta_{opt} = 3.7 + 0.69 \cdot |\lambda|$, whereas for $\lambda > 45°$ [18], gives: $\beta_{opt} = (3.7 + 0.69 \cdot |\lambda|) - 10^o$. However, in Ref. [20] the division is made at $\lambda = 65°$, giving, for $\lambda < 65°$, the formula $\beta_{opt} = 2.14 + 0.764 \cdot \lambda$, and for $\lambda \geq 65°$, $\beta_{opt} = 33.65 + 0.224 \cdot \lambda$. Talebizadeh et al. [21] give a general linear formula: $\beta_{opt} = 7.203 + 0.6804 \cdot \lambda$, and finally, Jacobson [22] provides a 3rd degree polynomial: $\beta_{opt} = 1.3793 + \lambda(1.2011 + \lambda(-0.014404 + 0.000080509\lambda))$. The accuracy of these formulas depends considerably on the assumption of clear skies (no cloud cover) throughout the year. This is especially significative for countries located above $45^o N$, most of which have long seasons of cloudiness. Frequently, non-optimal tilt angles are used in installations. For instance, increasing the number of PV modules may be better than just collecting the maximum energy per module (e.gr. a greater tilt angle may allow to install more modules in the same area [23]).

There are also many location-specific studies, which mix theoretical considerations, irradiation models and software products to compute the optimum β. For instance (and not intending to be exhaustive), Ullah et al. [24] use a solar irradiation transposition model, data from the National Renewable Energy Laboratory (NREL) [25] and the Energy Sector Management Assistance Program (ESMAP) [26] to compute that optimum for a site in Pakistan. Lv et al. [27] do the same for Lhasa (China), proposing the concept of effective solar heat collection, and using data from the Meteorological Data Set for China Building Thermal Environment Analysis [28]. Jafarkazemi et al. [29] use experimental data for different orientations ($0° \leq \gamma \leq 90°$) and tilt angles ($0° \leq \beta \leq 90°$) and data from the NASA Surface Meteorology and Solar-Energy model [30]. Skeiker [31] provides a mathematical model for determining the optimum β in several places in Syria, based on maximizing the extraterrestrial solar radiation for a specific date or period. Nafeh [32], on its part, maximizes the incident solar irradiance at solar noon on a PV array, for each day, month or year. MATLAB code is used in Refs. [24,27,29] for their computations.

Racking systems without solar tracker with monthly tilt update are scarcely studied [24,33,34]: are some references, but we have found no studies of these systems using daily tilt updates.

In summary, for racking systems without solar tracker, the present situation is as follows: there are studies for specific locations (which cannot be used elsewhere) and there are formulas whose accuracy depends greatly on the weather and climate conditions of the site (so, they are useful but not too precise).

The present study aims to compare the total energy obtained and the levelized cost of the produced electrical energy (LCOE) for the racking systems used in PVPS. For racking systems with solar tracker, we shall use the equations proposed in Ref. [12]. For those without solar tracker, we study three update frequencies of the tilt angle β: daily, monthly, and constant. Our analytical procedure uses an algorithm which maximizes the solar irradiation reaching the tilted surface for a given period of time, providing the optimum tilt angles for each day/month/whole year (depending on the update frequency). As a matter of fact, it can be applied to any update frequency (for instance, a different angle depending only on the hot/cold or dry/humid seasons). This analytical procedure is designed to obtain formulae which require the least number of parameters to determine optimum tilt angles. Our analysis is performed for 39 locations covering all the populated latitudes in the Northern Hemisphere and a large spectrum of longitudes.

The paper is organized as follows: the geographic characteristics of the cities under study are presented in Section 2. The proposed methodology is described and validated in Section 3; also in this section, the total (annual) energy obtained for each racking system and the valuation indicators are provided. Section 4 presents the results of the study. Finally, Section 5 summarizes the main contributions and conclusions of the paper.

2. Case study

In order to obtain a thorough assessment of the comparison by tilt update frequency across the World, we have selected 39 cities between 6° and 60° latitude North, covering a wide range of longitudes. We focus on the Northern hemisphere for two reasons: 90% of the World population lives in it [35] and it contains 60% of the Earth's available land. These locations are given in Table 1, together with their main geographical characteristics.

Table 1
Cities under study.

Id	City	Latitude	Longitude	Alt.(m)
1	Medellin (CO)	06°14′38″N	75°34 ′04″W	1469
2	Colombo (LK)	06°56′06″N	79°51′14″E	8
3	Bangkok (TH)	13°45′14″N	100°29 ′34″E	9
4	Dakar (SN)	14°41′34″N	17°26′52″W	12
5	Morelia (MX)	19°42′10″N	101°11 ′24″W	1921
6	El Paso (MX)	21°08′42″N	21°08′42″W	192
7	Karachi (PK)	24°52′01″N	67°01′51″E	14
8	Delhi (IN)	28°39′07″N	77°13′19″W	224
9	New Orleans (US)	29 °57′00″N	90°04′12″W	40
10	Cairo (EG)	30°29′24″N	31°14′38″W	41
11	Hefei (CN)	31°45′07″N	117°19 ′55″E	10
12	Djelfa (DZ)	34°20′34″N	03°16′15″E	1011
13	Alburquerque (US)	35 °05′02″N	35°05′02″W	1519
14	Handan (CN)	36°06′42″N	114°29 ′22″E	71
15	Desert Rock (US)	36 °37′00″N	97°43′37″W	1007
16	Almeria (ES)	36°50′07″N	02°24 ′08″W	22
17	Madrid (ES)	40°25′01″N	03°42′14″W	665
18	New York (US)	40°42′46″N	74° 00′21″W	26
19	Rock Springs (US)	40 °43′00″N	77°51′32″W	376
20	Chicago (US)	41°51′00″N	87°39 ′00″W	180
21	Rome (IT)	41°53′30″N	12°30′40″E	52
22	Toronto (CA)	43°39′14″N	79°23 ′13″W	106
23	San Marino (IT)	43 °56′45″N	12°27′28″E	363
24	Olympia (US)	47°02′42″N	122° 53′42″W	2
25	Nantes (FR)	47°13′08″N	01°33′14″W	16
26	Budapest (HU)	47°29′52″N	19° 02′23″E	111
27	Seattle (US)	47°36′22″N	122° 19′55″W	56
28	Freiburg (DE)	47°59′45″N	07° 50′56″E	282
29	Wien (AT)	48° 15′00″N	16°21′ 00″E	203
30	Valentia (IE)	51° 48′00″N	10°14′ 38″W	14
31	Saskatoon (CA)	52°07′56″N	106°40′08″W	454
32	Quebec (CA)	52° 28′33″N	71°49′33″W	477
33	Berlin (DE)	52° 31′27″N	13°24′37″E	37
34	Hamburg (DE)	53° 33′00″N	10°00′03″E	19
35	Alberta (CA)	55°00′03″N	115° 00′07″W	1045
36	Tartu (EE)	58° 15′00″N	26°43′48″E	70
37	S. Petersbutg (RU)	59°56′20″N	30°18′57″E	14
38	Lerwick (GB)	60°08′00″N	01°08 ′55″W	63
39	Helsinki (FI)	60°10′10″N	24° 56′07″E	23

3. Methodology

We use the following procedure: first, the solar irradiance at a specific latitude is estimated using the model proposed by Ref. [36]. Then, we estimate the amount of total irradiation reaching a tilted plane using a method derived from Ref. [12]. We then proceed to compute the optimum tilt angle of a racking system without solar tracker with different update frequencies (daily, monthly, and constant) using a novel method which we describe. The validation of this method is performed by comparing it to other procedures proposed in the literature. The equations providing the optimal tilts for each type of racking system with solar tracker are then presented, and, using the irradiations obtained in the first two steps, the values of total annual irradiation (MWh/m^2) are estimated for systems with trackers. Finally, we provide a detailed comparative study of LCOE for all the systems.

3.1. Step 1. model for estimating the solar irradiance

The total annual solar irradiation depends strongly on the geography and weather conditions of the site. In order to get a good estimation, one needs accurate site-specific data. The most common measurements in ground-level meteorological stations are the global and diffuse solar irradiances on a horizontal surface. Absent these values, one can only rely on theoretical estimations from irradiance models, and thus only approximate optimal values for the tilt can be expected.

Theoretical models for computing each component of the solar irradiance are manifold, and their accuracy differs by latitude [17]. One might cite the clear sky models of [37], satellite estimations [38], Angström's sunshine hours method [39], methods based on temperature records [40] …

In this work, we use the method presented in Ref. [36] to determine the hourly beam and diffuse horizontal solar irradiances. It takes into account the site's weather conditions for each day of the year. Using Hottel's model [41] for estimating the beam solar irradiance transmitted through clear atmospheres, Liu and Jordan's model [42] for determining diffuse solar irradiance for clear-sky, and Fourier series approximation for correcting those clear-sky models, it adapts them to the climatological conditions of the specific location. It has been validated for different climates, against actual data obtained from ground-level stations (the WRDC database [43]). For instance, in Wien (Austria), a place which we also cover in this paper, the R^2 coefficient for daily beam irradiation is 0.85713, and for daily diffuse irradiation it is 0.948112 (values which are generally considered proof of a very good fit [44]).

3.2. Step 2. Estimation of the amount of total irradiation on a tilted plane

The total solar irradiance (I_t) on a tilted surface is usually calculated as the sum of three components: the beam (I_{bt}), the diffuse (I_{dt}), and the ground reflected (I_{rt}) irradiances. The beam and reflected components are always computed the same way (using geometric considerations for the former and isotropic models for the latter), while there are multiple methods for the diffuse component. As the surface is tilted, and the irradiance is time-dependent, the following parameters are relevant: tilt angle, surface azimuth angle, and incident angle of the Sun.

Specifically: the *beam irradiance* is the component of the total irradiance which is received from the Sun without atmospheric scattering [12]; it can be estimated from the geometric relation between the horizontal plane and the tilted surface.

The *ground-reflected irradiance* is the fraction of the total irradiance reflected by the surface of the Earth and by any other surface (buildings, trees, etc.). It is essentially impossible to compute exactly, due to the many factors contributing to it [12]. However, one can assume [12,45], that the reflection on the ground of the beam and diffuse solar irradiances is isotropic. At the same time, it is also usually assumed [20] that the surroundings of the tilted surface have a constant diffuse reflectance, called ground reflectance (ρ_g), which depends on the type of ground surrounding the tilted surface. Muneer [46] computed its value for small surfaces. For instance, for weathered concrete $\rho_g = 0.22$; for dark surfaces of buildings (red brick, dark paints, etc.) $\rho_g = 0.27$; and for light surfaces of buildings (light brick, light paints, etc.) $\rho_g = 0.60$. For green vegetation and some soil types, one usually takes $\rho_g = 0.20$.

The *diffuse irradiance* is the component of the irradiance which has suffered scattering [12], so that its direction is hard to determine; it is divided into three components: isotropic, circumsolar and horizon brightening irradiances. The first one is received evenly from the entire sky dome. The second one is concentrated in the section of the sky around the Sun, whereas the last one is concentrated near the horizon and is most obvious in clear skies [47]. The models used to predict this solar irradiance on a tilted surface can be grouped in two families: isotropic and anisotropic.

(i) The isotropic models assume, as their name suggests, that the diffuse irradiance is only isotropic [45,48–50], so that it only depends on the tilt angle β of the surface.
(ii) Some anisotropic models assume that it is composed of an isotropic and a circumsolar component only [51–53], [54,55]. They depend mainly on β, the Sun height α_S, and the incidence angle θ_i, apart from other model-related parameters.
(iii) There are other anisotropic models in which it is assumed composed of an isotropic, a circumsolar, and a horizon brightening component [56–58]. They also depend on β, α_S, θ_i, and other model-related parameters.

Mehleri et al. [59] have compared several isotropic [45,48–50] and anisotropic models [51–53,56–58,60]. They conclude that the most accurate results were produced with the Liu and Jordan model [45]. Hence, it is commonly recommended for forecasting the diffuse irradiance at locations throughout the world [12,47,61].

The total irradiance $I_t(n, T, \beta)$ depends on the tilt angle β, the day of the year n and the solar time T, and is computed as:

$$I_t(n,T,\beta) = I_{bh}(n,T)\cdot\frac{\cos\theta_i}{\cos\theta_z} + I_{dh}(n,T)\cdot\left(\frac{1+\cos\beta}{2}\right) + (I_{bh}(n,T)+I_{dh}(n,T))\cdot\rho_g\cdot\left(\frac{1-\cos\beta}{2}\right) \quad (1)$$

where I_{bh} (W/m^2) is the beam irradiance on a horizontal plane, θ_z (°) is the zenith angle of the sun, θ_i (°) is the incident angle, I_{dh} (W/m^2) is the diffuse irradiance on a horizontal plane, β (°) is the tilt angle, and ρ_g (dimensionless) is the ground reflectance. Solar time is the time used in the sun-angle relations, and in this work we set the time variable to mean Solar time. The incident angle of the Sun θ_i (°) on a tilted surface can be determined following [12] as (notice that in all our formulas we assume the azimuth angle to be $\gamma = 0$):

$$\cos\theta_i = \sin\delta\cdot\sin\lambda\cdot\cos\beta - \sin\delta\cdot\cos\lambda\cdot\sin\beta + \cos\delta\cdot\cos\lambda\cdot\cos\beta\cdot\cos\omega + \cos\delta\cdot\sin\lambda\cdot\sin\beta\cdot\cos\omega \quad (2)$$

where δ is the declination, λ the latitude, β the tilt angle, and ω the hour angle. When using equation (2), it is necessary to take into account that the incidence angle might exceed 90° (i.e. the Sun is behind the surface and the Earth is not blocking the Sun).

Using *eq.* (1), we can compute, by direct integration from sunrise to sunset, the total irradiation on a tilted surface $H_t(n, \beta)$ (Wh/m^2) for each n day of the year, and each tilt angle β (where $T_R(n)$ is the sunrise time and $T_S(n)$ the sunset):

$$H_t(n,\beta) = \int_{T_R(n)}^{T_S(n)} I_t(n,T,\beta)dT \quad (3)$$

This function $H_t(n, \beta)$ is what allows us to compute the total annual irradiation on a tilted plane depending on the tilt settings.

It is at this point that a discretization of the tilt angle is necessary. We have divided the range [0, 90] (°) into 900 intervals of width 0.1 (°). The 2-variable function $H_t(n, \beta)$ (Wh/m^2) for the case of Almeria ((16), Spain, with latitude 36°50′07″N, longitude 02°24′08″W and altitude 22 (m)) is shown in Fig. 1.

3.3. Step 3. Determination of the optimum tilt angle for racking systems without solar tracker

We now compute the total irradiation on a racking system without solar tracker, for different update frequencies. We consider, in what follows, 3 different frequencies: (1) Daily, (2) Monthly, and (3) Yearly (constant tilt).

3.3.1. Daily tilt updates

In the analytical procedure we propose, we assume in this step that the tilt of the PV system is updated daily. Our method requires computing, for each day n, the optimal tilt angle β, which we shall call $\beta^d_{opt}(n)$. Consider, in Fig. 1, each section of the surface $H^n_t(\beta)$ for a fixed n (i.e. the function of the variable β which gives the total solar irradiation for that day n if the tilt angle is β). We need to find, for that section, the tilt angle $\beta^d_{opt}(n)$ such that irradiation for that day:

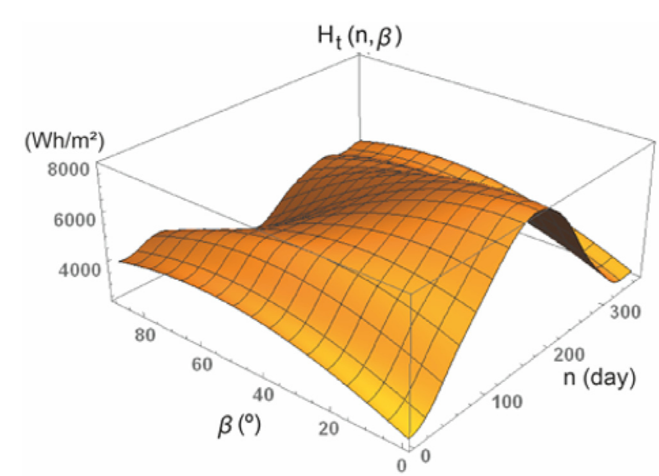

Fig. 1. Total daily solar irradiation on a tilted surface $H_t(n, \beta)$.

$$H_t^n(\beta_{opt}^d(n)) = \max_{\beta} \; H_t^n(\beta) \tag{4}$$

In some sense, we are finding the "crest" point for each n of the function $H_t(n, \beta)$. In Fig. 2 we show how β_{opt}^d varies throughout the year for our chosen location (nr. 16, Almeria), and in Fig. 3 we plot the "crest" of values of $H_t(n, \beta)$ over those optima. The area under this crest is the maximum energy than can be produced during a year when the tilt is modified daily.

The shaded area in Fig. 3 (maximum energy under daily update of β) is, for Almeria (Spain):

$$\int_1^{365} H_t\left(n, \beta_{opt}^d(n)\right) dn = 2.22145 \times 10^6 \; (\text{Wh/m}^2) \tag{5}$$

The validation of the proposed method is done comparing our results to those obtained using the well-know formula of Duffie [12] for East-West trackers with daily update. Notice, by the way, that in this case, Duffie's formula requires the azimuth γ of the receiver to change: it must be 0° if $|\lambda - \delta| > 0$ and 180° if $|\lambda - \delta| \leq 0$, δ being the declination. Duffie's daily formula is given then by:

$$\beta_{opt} = |\lambda - \delta| \tag{6}$$

Table 2 contains the values of total annual irradiation (MWh/m^2) estimated using Duffie's formula with daily update (H_{Duffie}^d) and the proposed method ($H_{proposed}^d$).

The difference ratio in total annual irradiation with daily update is plotted in Fig. 4. Notice that, in what follows, we shall refer to each city by their Id number (first column of Table 1). The values are % with respect to the Duffie's method, that is:

$$\frac{H_{proposed}^d - H_{Duffie}^d}{H_{Duffie}^d} \cdot 100 \tag{7}$$

Comparing our method with Duffie's daily method (6), using Fig. 4, we can conclude (apart from our method being consistently better than Duffie's):

(i) The present model can be considered validated, as these deviations are not greater than 2.5%.
(ii) For locations with $\lambda < 45°$, the improvement is slight: between 0.03% and 0.79%.

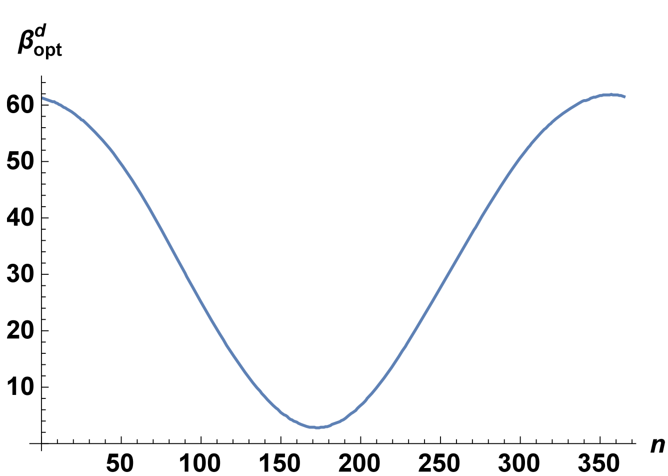

Fig. 2. Plot of $\beta_{opt}^d(n)$.

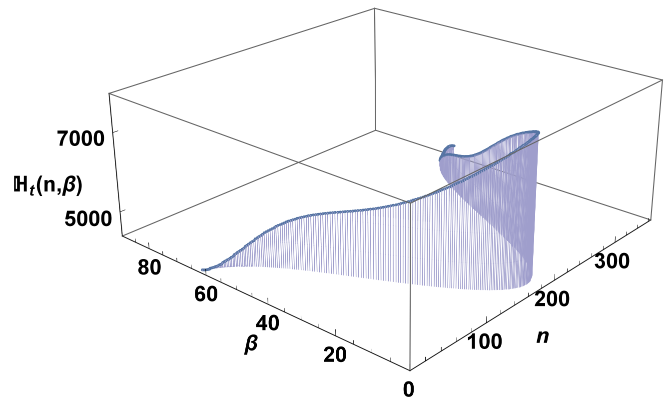

Fig. 3. Plot of $H_t\left(n, \beta_{opt}^d(n)\right)$.

(iii) However, when $\lambda > 45°$, the improvements are larger, up to 2.44% in Lerwick (nr. 38).

In order to try and explain this improvement, we have plotted, in Fig. 5, the daily values of β_{opt}^d (proposed method) and Duffie's daily optimum tilts, in the case of Almeria (nr. 16). Notice the remarkable difference from the Spring to the Autumn equinox, where our method (because it takes into account the meteorological conditions) suggests a decrease in the tilt angle with respect to Duffie's: Almeria is one of the sunniest places in Europe. In other places, a similar behavior is noticeable, although the major difference may take place at other times (Spring, Winter …), and the optimum tilt angle is adjusted according to the climatic and weather conditions of each location.

3.3.2. Monthly tilt updates

We now consider, in our analytical method, a PV system whose tilt angle is modified monthly. We have to divide the period into the 12months and solve as many optimization problems of the form:

$$H_t^{\beta,m} = \int_{f(m)}^{l(m)} H_t(n, \beta) dn; \; \max_{\beta} \; H_t^{\beta,m}; \; m = 1, \ldots, 12 \tag{8}$$

where $f(m)$ and $l(m)$ are the first and last days of each month, respectively. Calling $\beta_{opt}^m(m)$ the optimum β for each month m, we obtain, for Almeria (nr. 16), the 12 values (in degrees):

$$\beta_{opt}^m(m) = [59.1, 51.0, 37.9, 22.4, 9.8, 3.5, 6.4, 17.3, 31.7, 46.0, 56.6, 61.4] \tag{9}$$

and the maximum annual irradiation is now:

$$\sum_{m=1}^{12} \max_{\beta} \; H_t^{\beta,m} = 2.21878 \times 10^6 \; (\text{Wh/m}^2) \tag{10}$$

Table 3 contains the values of total annual irradiation (MWh/m^2) estimated using the proposed method with monthly update.

3.3.3. Constant tilt (year-long optimization)

Finally, we consider that the tilt angle of the PV system is constant. When this happens (so that, most likely, the PV system is totally rigid), the volume underneath the graph of our two-variable function is given by the double integral

Table 2
Estimated total annual irradiation with daily update (MWh/m^2).

City	Duffie	Proposed	City	Duffie	Prop.	City	Duffie	Prop.
Medellin	1.8947	1.8953	Handan	1.5516	1.5620	Seattle	1.4199	1.4319
Colombo	2.0977	2.0989	Desert Rock	2.4620	2.4743	Freiburg	1.4287	1.4396
Bangkok	1.9543	1.9558	Almeria	2.2127	2.2214	Wien	1.3746	1.3886
Dakar	2.3006	2.3038	Madrid	1.9696	1.9806	Valentia	1.0721	1.0907
Morelia	2.2865	2.2931	New York	1.6480	1.6575	Saskatoon	1.4449	1.4585
El Paso	1.8150	1.8178	Rock Springs	1.4717	1.4819	Quebec	1.1933	1.2091
Karachi	2.3433	2.3477	Chicago	1.5843	1.5950	Berlin	1.2026	1.2212
Delhi	2.0695	2.0751	Rome	1.8636	1.8737	Hamburg	1.1981	1.2115
New Orl.	1.9035	1.9096	Toronto	1.4901	1.5018	Alberta	1.3638	1.3799
Cairo	2.3859	2.3939	San Marino	1.5954	1.6080	Tartu	1.0698	1.0890
Hefei	1.4332	1.4420	Olympia	1.3562	1.3687	S. Peters.	1.1369	1.1530
Djelfa	2.2755	2.2864	Nantes	1.5015	1.5121	Lerwick	0.8429	0.8666
Alburq.	2.3844	2.3969	Budapest	1.2980	1.3145	Helsinki	1.0724	1.0899

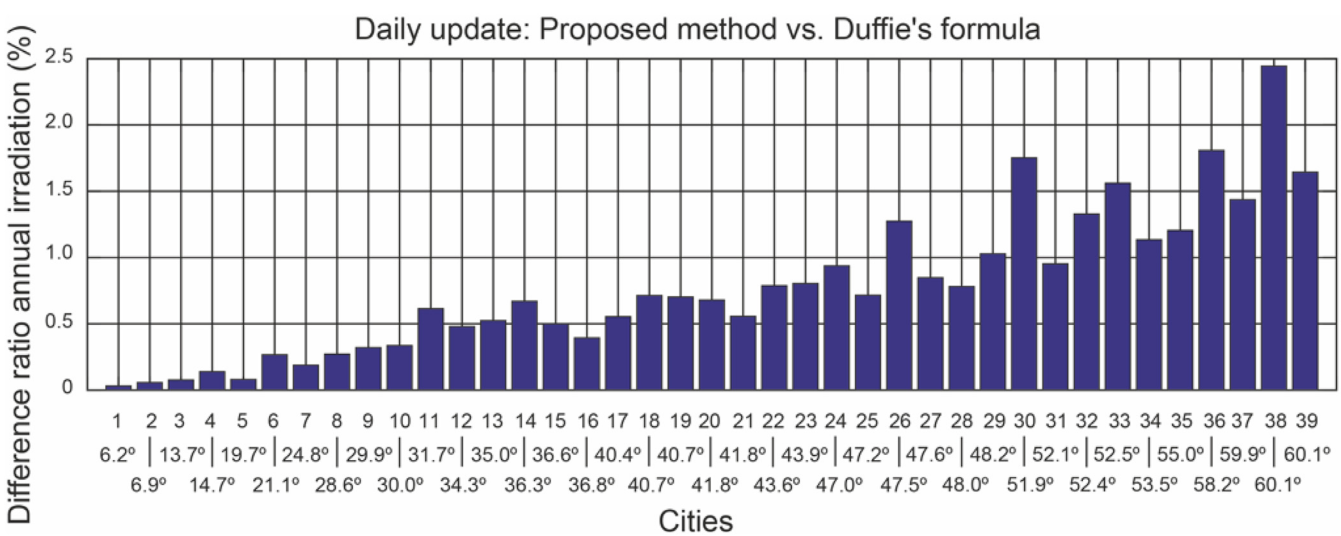

Fig. 4. Difference ratio of total annual irradiation between proposed daily update and Duffie's formula.

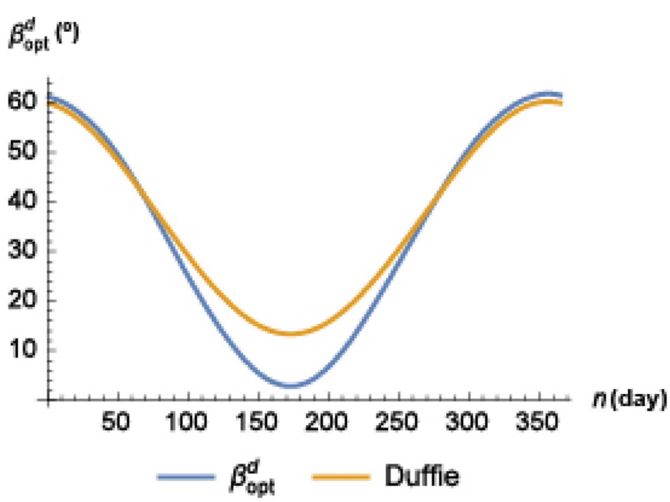

Fig. 5. Daily values of $\beta^d_{opt}(n)$ and Duffie's formula (6).

$$\iint_D H_t(n,\beta)\,dn\,d\beta \qquad (11)$$

where D is the rectangle $D : [1, 365] \times [0, 90]$. In what follows, the reader will notice that our method is essentially, the application of Cavaleri's principle of integral calculus, whose proper generalization is Fubini's Theorem [62]. In order to compute the optimal year-long constant tilt β_{opt}, we discretise the interval [0, 90] as above and compute the integral for each of the values provided by that discretization. Following the Cavalieri idea, we are evaluating:

Table 3
Estimated annual irradiation, monthly tilt updates (MWh/m^2).

City	Irrad.	City	Irrad.	City	Irrad.
Medellin	1.8940	Handan	1.5606	Seattle	1.4303
Colombo	2.0971	Desert Rock	2.4708	Freiburg	1.4380
Bangkok	1.9543	Almeria	2.2188	Wien	1.3871
Dakar	2.3015	Madrid	1.9783	Valentia	1.0896
Morelia	2.2906	New York	1.6557	Saskatoon	1.4566
El Paso	1.8165	Rock Springs	1.4804	Quebec	1.2076
Karachi	2.3453	Chicago	1.5933	Berlin	1.2200
Delhi	2.0729	Rome	1.8717	Hamburg	1.2102
New Orleans	1.9075	Toronto	1.5002	Alberta	1.3780
Cairo	2.3913	San Marino	1.6063	Tartu	1.0878
Hefei	1.4410	Olympia	1.3673	S. Petersburg	1.1517
Djelfa	2.2836	Nantes	1.5103	Lerwick	0.8656
Alburquerque	2.3936	Budapest	1.3133	Helsinki	1.0885

$$H_t^{\beta} = \int_1^{365} H_t(n,\beta)dn \tag{12}$$

And we seek β_{opt}^{y} such that:

$$H_t^{\beta_{opt}^{y}} = \max_{\beta} \; H_t^{\beta} \tag{13}$$

just by exhaustive search. In order to clarify the exposition, we show again the case of Almeria (nr. 16). Fig. 6 contains the plot of H_t^{β} against β: there is a clear maximum near 30°, which for a discretization in tenths of angle, is actually $\beta_{opt}^{y} = 30.3^{o}$. In Fig. 7 we plot $H_t(n,\beta)$ only for this specific value $\beta = \beta_{opt}^{y}$. The shaded area represents the maximum possible total annual irradiation with a fixed tilt. For this value of β_{opt}^{y}, we obtain $\max_{\beta} \; H_t^{\beta} = 2.1084\ 10^6$ (Wh/m^2).

There exist multiple elementary formulas for computing the tilt angle as rule of thumb by solar energy system installers [18–21]. However, the validation of the proposed method is done using Jacobson's formula [22], which is better than a simple linear interpolation. As a matter of fact, Jacobson's model is considered a good fit for real-life PV systems [63], and it has been used extensively [64–66]. Jacobson's formula for a constant optimum tilt angle depending on the latitude λ is [22]:

$$\beta_{opt} = 1.3793 + \lambda(1.2011 + \lambda(-0.014404 + 0.000080509\lambda)) \tag{14}$$

Fig. 8 shows the annual (i.e. constant) optimum tilt angle β_{opt}^{y} (proposed method) for the 39 cities and the one computed using Jacobson's formula, Eq. (14) [22].

Table 4 contains the values of total annual irradiation (MWh/m^2) estimated using Jacobson's formula ($H_{Jacobson}^{y}$) and with the proposed method ($H_{proposed}^{y}$). The difference ratio in total annual irradiation with constant tilt is shown in Fig. 9. The values are %, with respect to the Jacobson's method, that is:

$$\frac{H_{proposed}^{y} - H_{Jacobson}^{y}}{H_{Jacobson}^{y}} \cdot 100 \tag{15}$$

From Figs. 8 and 9 we can easily conclude:

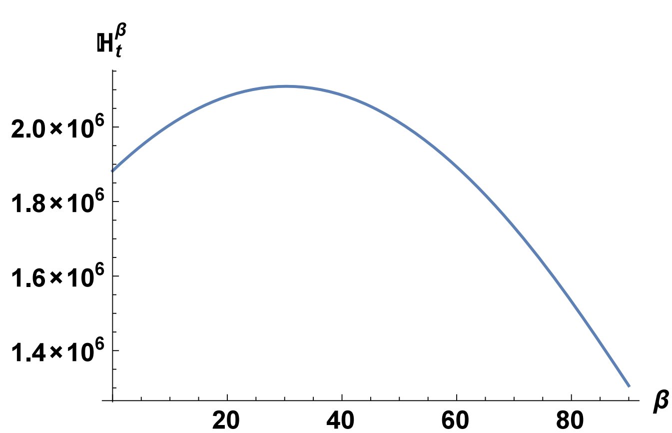

Fig. 6. Plot of H_t^{β}.

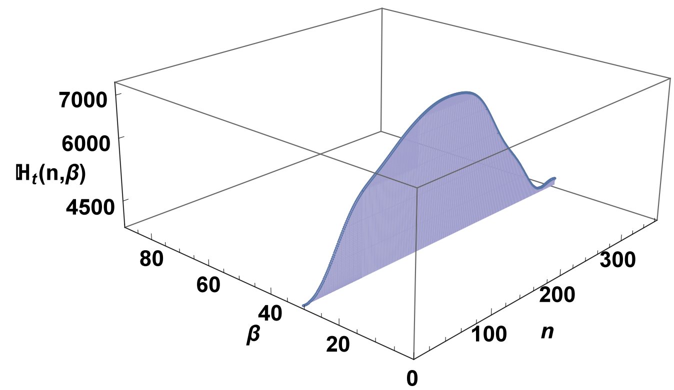

Fig. 7. Annual irradiation for β_{opt}^{y}.

(i) The present model can be considered validated, as these deviations are not greater than 0.35%.
(ii) As regards the rate of improvement in annual irradiation, for locations with $\lambda < 45°$, it is up to 0.34%, whereas for $\lambda \geq 45°$, the increase is up to 0.35% in Budapest (nr. 26).
(iii) Our main remark is that there are many locations for which the difference between our optimum tilt angle and Jacobson's formula can be large (by which we mean larger than 5°); this stresses the importance of using a method which takes into account the meteorological features of each place. Notice, for example, Hefei (nr. 11), where our estimate is 21.6, Jacobson's is 27.5.

3.4. Step 4. Racking systems with solar tracker

We now study racking systems with solar tracker, whose orientation is continuously updated. These are classified according to their axes of motion (either two or one, and the latter depend on their orientation). Table 5 summarizes the different types and the formulas for their tilt and azimuth angles, following (with a different notation for the polar axis case) [12]. Finally, Table 6 contains the estimated values of total annual irradiation (MWh/m²) for each of these systems.

3.5. Step 5. Efficacy assessment

We evaluate the efficacy of each racking system in relation to the best one (dual-axis tracker) in two aspects: the relative loss of energy production and the levelized cost of the electrical energy (LCOE) produced. The trackers we consider are: (a) single axis with Polar tracker, (b) with North-South axis, (c) with East-West axis, (d) no tracker with daily update, (e) no tracker with monthly update, and (f) no tracker with constant tilt. Whenever an * appears in any of the formulas below, it should be replaced with the corresponding type.

3.5.1. Step 5.1 Energy loss ratio

We just compute the difference between the energy absorbed by the specific system under study and the dual-axis tracker, as a % of energy:

$$Energy\ loss = \frac{H_{*} - H_{2-axis}}{H_{2-axis}} \cdot 100 \tag{16}$$

Where the subindex * stands, as above, for the corresponding tracker (Polar, North-South, etc.).

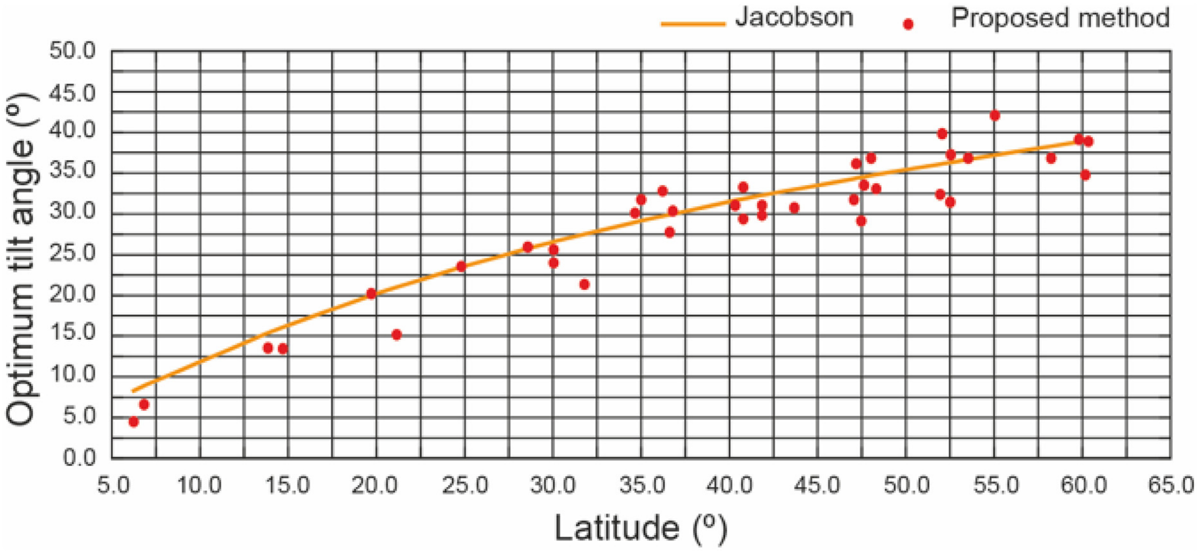

Fig. 8. Optimum tilt angle for cities under study and Jacobson's formula.

Table 4
Estimated annual irradiation, Jacobson and fixed (constant) tilt (MWh/m^2).

City	Jacob.	Fixed	City	Jacob.	Fixed	City	Jacob.	Fixed
Medellin	1.8274	1.8299	Handan	1.4992	1.4999	Seattle	1.3777	1.3779
Colombo	2.0197	2.0209	Desert Rock	2.3276	2.3291	Freiburg	1.3796	1.3799
Bangkok	1.8843	1.8852	Almeria	2.1084	2.1084	Wien	1.3403	1.3408
Dakar	2.2001	2.2019	Madrid	1.8889	1.8891	Valentia	1.0533	1.0547
Morelia	2.1772	2.1772	New York	1.5816	1.5817	Saskatoon	1.3887	1.3901
El Paso	1.7487	1.7547	Rock Spr.	1.4209	1.4217	Quebec	1.1566	1.1567
Karachi	2.2398	2.2398	Chicago	1.5305	1.5312	Berlin	1.1886	1.1907
Delhi	1.9881	1.9881	Rome	1.7954	1.7958	Hamburg	1.1701	1.1701
New Orl.	1.8217	1.8219	Toronto	1.4442	1.4450	Alberta	1.3060	1.3095
Cairo	2.2764	2.2779	San Marino	1.5438	1.5448	Tartu	1.0524	1.0526
Hefei	1.3915	1.3961	Olympia	1.3200	1.3209	S. Peters.	1.1232	1.1232
Djelfa	2.1635	2.1636	Nantes	1.4477	1.4481	Lerwick	0.8367	0.8381
Alburq.	2.2533	2.2546	Budapest	1.2772	1.2811	Helsinki	1.0562	1.0562

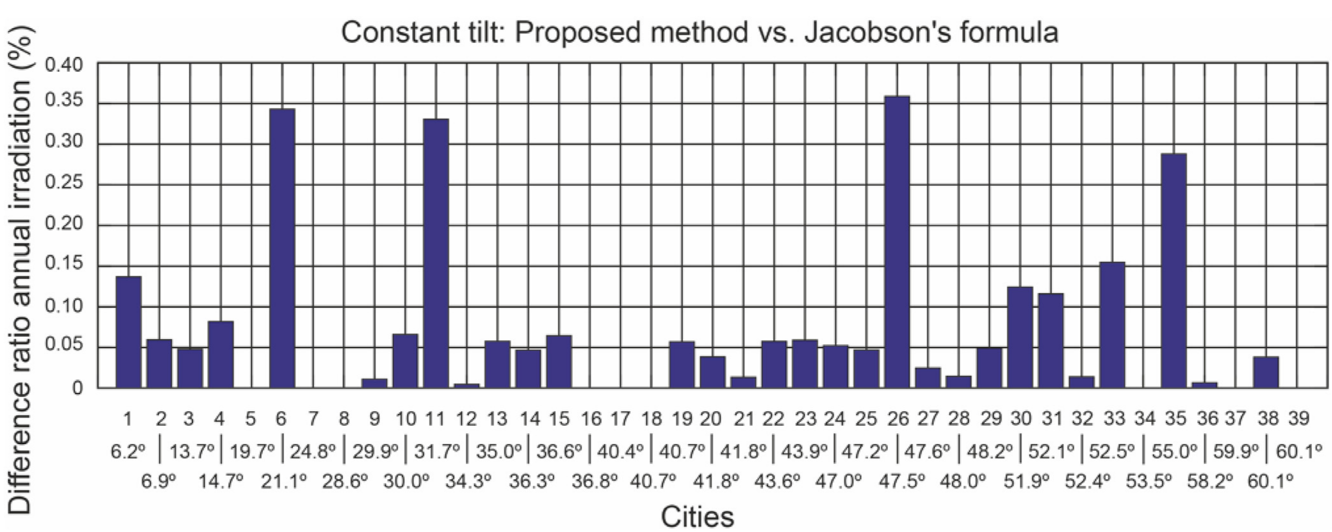

Fig. 9. Difference ratio in total annual irradiation with constant tilt: proposed method vs. Jacobson's formula.

3.5.2. Step 5.2. LCOE

The Levelized Cost of Electrical Energy (LCOE) is a standardized value (USD/kWh), defined as the ratio between the life-cycle cost of the PV system and the energy produced during its whole operative life. The following definition is given in Ref. [67]:

Table 5
Parameters for the types of solar tracker [12].

Tracker	Tilt angle	Surface azimuth angle
Dual-axis	θ_z	γ_s
Polar axis	$\arccos(\cos\omega\cos\lambda)$	$\gamma=\gamma^*$ if $\lvert\omega\rvert<90^o$; $\gamma=-180^o-\gamma^*$ if $\omega<90^o$; $\gamma=180^o-\gamma^*$ if $\omega>90^o$; $\gamma^*=sign(\omega)\arccos\frac{1}{\sqrt{1+\frac{\tan^2\omega}{\sin^2\lambda}}}$
N–S axis	$\arctan(\tan\theta_z\lvert\cos(\gamma-\gamma_s)\rvert)$	$90°(\gamma_s>0)\ or -90°(\gamma_s\le 0)$
E-W axis	$\arctan(\tan\theta_z\lvert cos\gamma_s\rvert)$	$0°(\lvert\gamma_s\rvert<90°)\ or\ 180°(\lvert\gamma_s\rvert\ge 90°)$

Table 6
Estimated annual irradiation for systems with solar tracker (MWh/m^2).

City	Dual-axis	Polar-axis	NS-Single	EW-Single
Medellin	2.1908	2.1371	2.1340	1.8968
Colombo	2.4670	2.4033	2.3951	2.1015
Bangkok	2.2366	2.1788	2.1505	1.9543
Dakar	2.7499	2.6682	2.6310	2.3114
Morelia	2.8536	2.7608	2.6826	2.3143
El Paso	2.1120	2.0552	2.0203	1.8221
Karachi	2.7917	2.7039	2.5880	2.3567
Delhi	2.4339	2.3627	2.2453	2.0798
New Orleans	2.2721	2.1997	2.0893	1.9186
Cairo	2.9540	2.8585	2.7238	2.4161
Hefei	1.6049	1.5602	1.5099	1.4374
Djelfa	2.8689	2.7704	2.5916	2.3150
Alburquerque	3.1041	2.9949	2.7713	2.4364
Handan	1.7688	1.7130	1.6163	1.5614
Desert Rock	3.2269	3.1144	2.8671	2.5185
Almeria	2.7936	2.6998	2.5004	2.2521
Madrid	2.5898	2.5007	2.3029	2.0891
New York	1.9769	1.9093	1.7595	1.6695
Rock Springs	1.7752	1.7160	1.6066	1.4958
Chicago	1.9324	1.8675	1.7436	1.6118
Rome	2.3314	2.2549	2.0890	1.9021
Toronto	1.8004	1.7389	1.6216	1.5166
San Marino	1.9685	1.9003	1.7716	1.6307
Olympia	1.6575	1.5985	1.4847	1.3867
Nantes	1.8539	1.7905	1.6165	1.5339
Budapest	1.5574	1.5038	1.4231	1.3256
Seattle	1.7561	1.6938	1.5574	1.4542
Freiburg	1.7819	1.7214	1.5554	1.4638
Wien	1.6773	1.6186	1.4971	1.4059
Valentia	1.2569	1.2054	1.1257	1.0970
Saskatoon	1.8407	1.7695	1.5747	1.4944
Quebec	1.4662	1.4075	1.2742	1.2290
Berlin	1.4581	1.4028	1.3121	1.2366
Hamburg	1.4950	1.4392	1.3028	1.2361
Alberta	1.7468	1.6761	1.4693	1.4186
Tartu	1.3316	1.2714	1.1590	1.1166
S. Petersbutg	1.4877	1.4274	1.2830	1.1982
Lerwick	1.0587	1.0094	0.8975	0.9254
Helsinki	1.3824	1.3203	1.1926	1.1292

$$LCOE=\frac{\sum_{i=0}^{I}\left[C_i\Big/(1+r)^i\right]}{\sum_{i=0}^{I}\left[E_i\Big/(1+r)^i\right]} \quad (17)$$

where, for each year i, C_i is the net cost (USD) of the project in that year, E_i is the total energy output (in that year, in kWh), I is the lifetime of the project (years) and r the discount rate. This E_i can be computed, for PV systems, as

$$E_i=S_i\bullet\eta\bullet(1-d)^i \quad (18)$$

where S_i is the availability of solar resources in year i (kWh), η is the performance factor, and d is the annual degradation rate. Thus, the LCOE gathers in a single value the initial investment cost, the operation and maintenance costs, the interest expenditure if financed, and, on the other hand, the energetic output.

Obviously, the LCOE depends on site-specific parameters as power capacity, PV technology, location…In order to provide a reasonable assessment, we are going to assume from now on, as elsewhere in the literature, the following:

(i) *Initial investment cost.* As explained in the introduction, dual axis tracking systems require a greater initial investment than single-axis or fixed systems, with a premium of 40–50% over fixed systems, and $20-25\%$ over single-axis ones [8]. In this paper, we assume respective premiums of 50% and 25%.
(ii) *Operation and maintenance costs.* Despite the lack of standardization [10] for this value, the National Renewable Energy Laboratory recommends assuming an annual cost of 0.5% of the total initial cost for large systems, and 1% for small ones. Moreover, Mortensen [68] suggests that operation and maintenance costs with tracking systems are double those of fixed-tilt ones. We are going to assume 0.5% of the initial investment for systems with tracking, and 0.25% for systems without.
(iii) *Interest costs (financing).* We are not taking into account this value, as it is outside the scope of any control.
(iv) *Discount rate.* For the same reasons, we are not going to take into account this value (i.e. $r=0$), as these are country- and time-specific.
(v) *Total electrical energy output.* This value is directly proportional to the availability of solar resources at each location. We consider the same performance factor and degradation rate for all the systems.
(vi) *Project lifetime.* We take a fixed value of 20 years [67].

From the considerations above, it follows that location is quite relevant in the computation of the LCOE. We are going to use the following ratio to compare the LCOE values for single-axis and fixed-tilt systems to two-axis systems ($LCOE_{2-axis}$):

$$\eta_{LCOE}=\frac{LCOE_*}{LCOE_{2-axis}} \quad (19)$$

where, as above, * is one of the different tracking systems we are comparing. Notice that an η_{LCOE} value greater than 1 implies that the corresponding tracking system is *less* efficient than the dual-axis system.

4. Results and discussion

Based on the methodology presented above, the Computer

Algebra System Mathematica© was used for computing the total annual irradiation at 39 sites covering a large part of the Northern Hemisphere, as well as the total energy produced by the different PV systems with or without solar tracking, with optimum tilt angles. The PVGIS [69] database was used to obtain the irradiation data with which to compute the estimated irradiance. The LCOE is the metric used to analyze their efficiency. The remainder of this section contains the outputs of our computations and the comparison of each system with the best one, the dual-axis tracker.

For a specific location, we start by collecting the satellite estimations of monthly-averaged global and diffuse solar irradiations received on a horizontal surface. We use the publicly available PVGIS database [69], but any other source is equivalent. From these monthly values, we compute, using Fourier analysis and the classic clear-sky beam and diffuse irradiation models [36] (in this paper we apply the Hottel and Liu Jordan models, respectively), hourly distributions for the beam and diffuse solar irradiances. By integration, taking into account that β can be updated hourly, daily, monthly or be constant throughout the year, we obtain the total irradiation for each day of the year and the different tilt upgrade frequencies. A main advantage of our methodology is that it takes into account the main environmental conditions of the site.

4.1. Evaluation of energy losses

In this section we calculate the losses in produced energy of the different systems with respect to the dual-axis tracker. Fig. 10 contains this comparison using Eq. (16).

Fig. 10 suggests the following conclusions:

(i) Obviously, dual-axis tracker systems yield the best performance everywhere.
(ii) The maximum loss of absorbed energy for the polar axis tracker is 3.46% for locations with $\lambda < 45^\circ$, and 4.65% for locations with $\lambda \geq 45^\circ$.
(iii) For North-South aligned axis trackers, the maximum losses are 11.15% for $\lambda < 45^\circ$ and 15.88% for $\lambda \geq 45^\circ$.
(iv) For East-West aligned axis trackers, these maxima are 21.95% and 19.45%, respectively.
(v) The least efficient systems is the constant-tilt one, with maximum (relative) loss of 27.82% at Desert Rock (nr. 15).

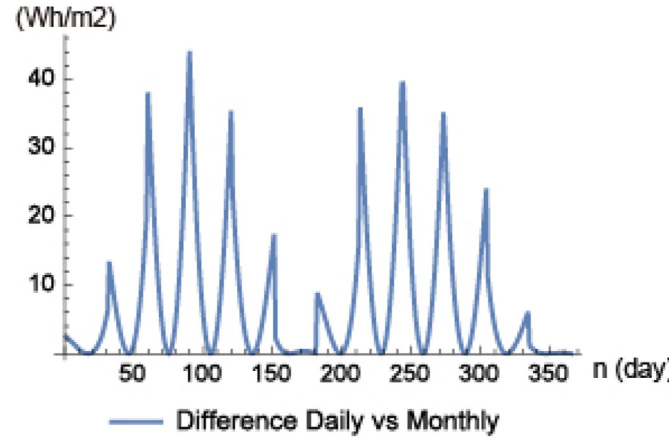

Fig. 11. Difference in irradiation between daily and monthly tilt updates.

One of the most striking results (in our view) is the surprisingly good results obtained using the system without tracker with monthly tilt update. Notice also, from Fig. 10 that:

(i) Updating the tilt angle daily is only marginally better than doing so monthly.
(ii) The spread of this improvement is the interval 0.07%–0.14% (Bangkok (nr. 3) and Desert Rock (nr. 15)), respectively.
(iii) The reason for this small difference can be glimpsed in Fig. 11, which plots the daily absolute differences in irradiation between the daily and the monthly update method, in the specific case of Almeria (nr. 16). There is only a significant

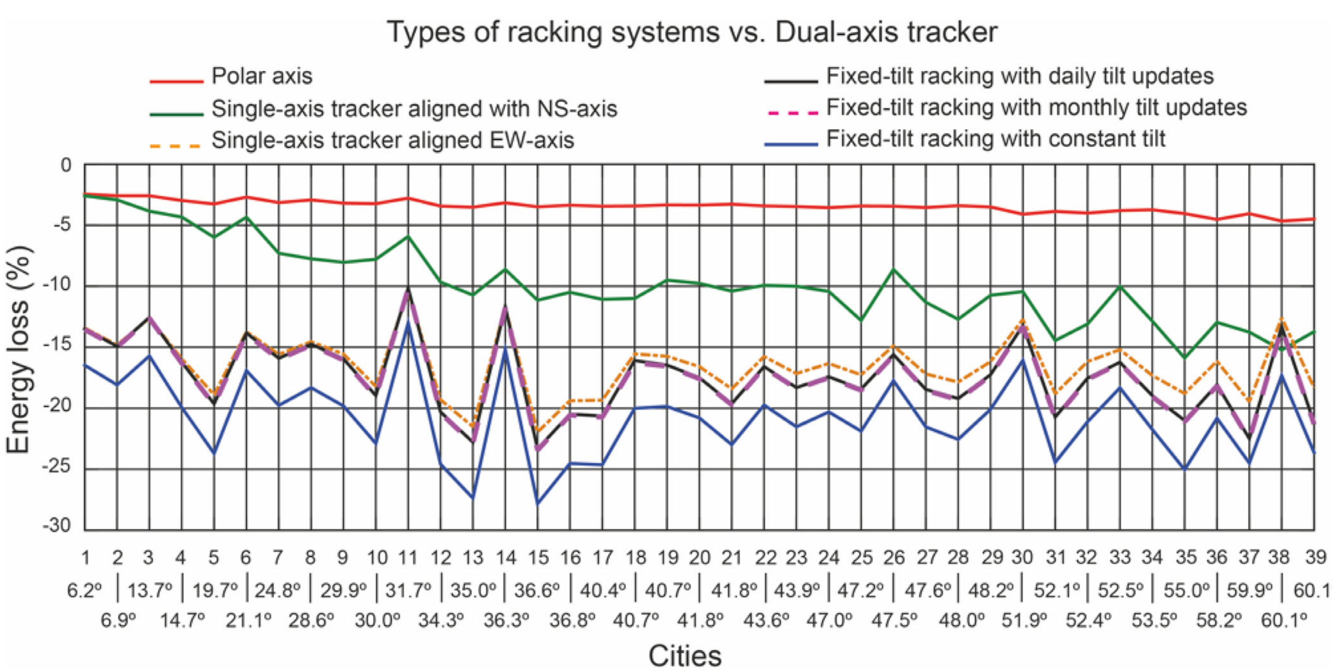

Fig. 10. Ratio of energy loss with respect to the dual-axis tracker. Notice that the daily and monthly plots overlap.

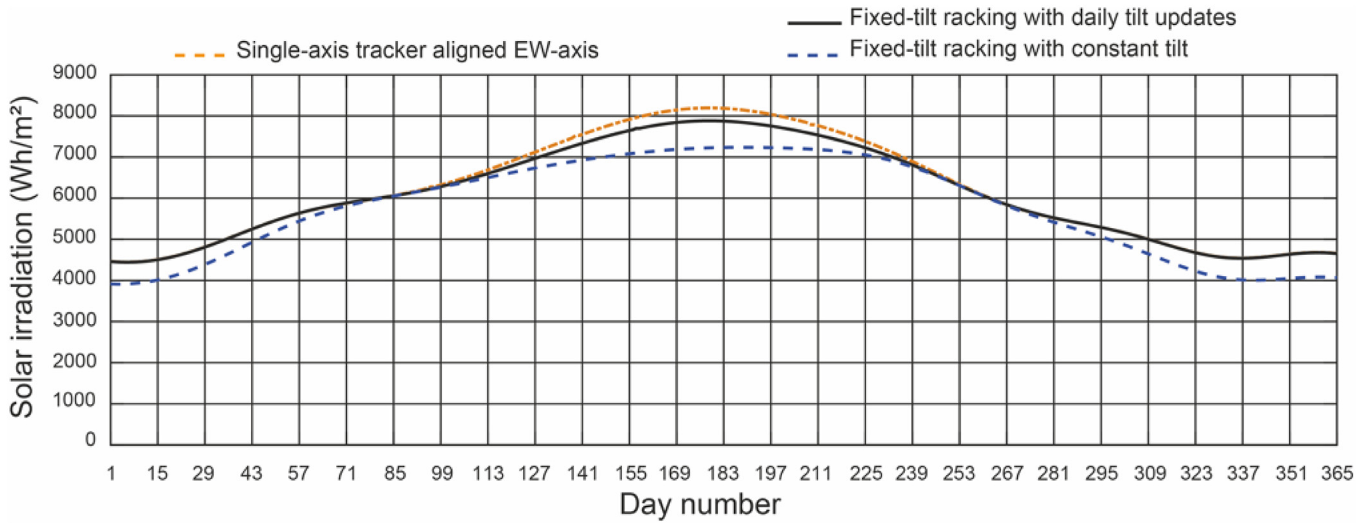

Fig. 12. Daily irradiation in Almeria (nr. 16).

difference on the first days of each month, and this does not reach even 1% (less than 50 Wh/m^2 of daily irradiation).

On the other hand, the improvement in energy production, with respect to the constant-tilt system, if the is updated monthly, is between 2.53% (St. Petersbutg, nr. 37) and 6.16% (Alburquerque, nr. 13).

Fig. 12 shows the total daily solar irradiation harvested throughout the year in Almeria (nr. 16), using single axis trackers with East-West axis, and trackerless systems with daily update and with constant tilt. Clearly, the main difference takes place during the Summer and, remarkably, the first two systems give essentially the same values except for the central days of the year. Constant-tilt systems show a very good efficiency near the equinoxes but also great losses at other times.

4.2. Evaluation of the systems wit respect to the LCOE

We now compare the LCOE of all the systems, taking as baseline the most energy-efficient (the dual-axis tracker), by computing the ratio between the LCOE of each of the others and this one. The summary results are shown in Fig. 13, for which Eq. (19) has been used.

The following conclusions can be inferred from Fig. 13:

(i) The most efficient system with respect to LCOE is the one without solar tracker with constant tilt (no update whatsoever). Despite being the one which generates the least energy, it also requires the least initial investment. The ratio of LCOE with respect to the dual-axis tracker varies between 0.76 (Hefei, nr. 11) and 0.91 (Alburquerque, nr. 13).

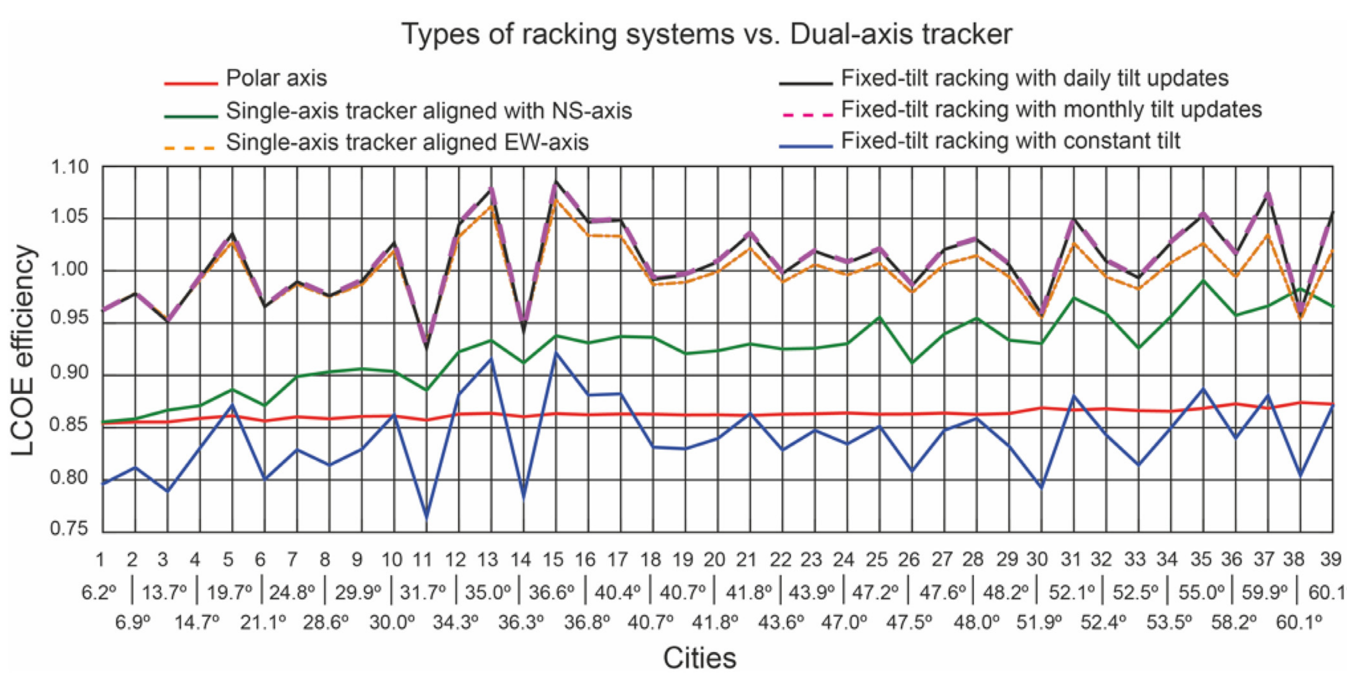

Fig. 13. LCOE efficiency with respect to the dual-axis tracker. Notice that the daily and monthly plots overlap.

(ii) The single-axis system with polar axis shows a good LCOE efficiency, and notably, its ratio with respect to the dual-axis tracker is essentially the same for all latitudes (between 0.85 and 0.87).
(iii) The N–S oriented single-axis system has also a good LCOE efficiency, but its improvement ratio depends greatly on the latitude: between 0.85 (Medellin, nr. 1) and 0.99 (Alberta, nr. 35).
(iv) Single-axis systems with East-West alignment, and systems without tracker but daily or monthly updates are the worst in terms of this metric. They are the ones producing the least energy (except for the constant tilt) and their initial investment does not make up for that loss.

The sensitivity of the model is measured as the influence of the initial investment cost on LCOE. Notice that the initial investment cost of the dual-axis tracker is greater than the rest of the systems. We are going to use the initial investment costs specified in Section 3.5: there is a premium in the dual tracker of 40–50% over fixed systems and a of 20–25% over single-axis ones [8]. Fig. 14 illustrate our sensitivity analysis for Almeria (nr. 16). The following conclusions can be inferred:

(i) Regardless of the initial investment cost, the polar axis, the single-axis tracker aligned with NS-axis and the fixed-tilt racking with constant tilt have always a good LCOE.
(ii) The single-axis tracker aligned with EW-axis, the fixed-tilt racking with daily tilt updates, and the fixed-tilt racking with monthly tilt updates have always a bad LCOE.
(iii) The best LCOE is reached when the initial investment of the dual-axis system is minimal with respect to the single-axis one, and when the initial investment of the dual axis-system is maximal with respect to the fixed system.
(iv) The worst LCOE happens when the initial investment of the dual-axis system is maximal with respect to the single-axis, and when the initial investment of the dual-axis system is minimal with respect to the fixed one.

5. Conclusions

We have carried out a a comparative study of the efficiency of different racking systems of photovoltaic power systems in 39 locations in the North Hemisphere covering a wide range of latitudes.

In order to do so, a new methodology for computing the optimum tilt angle for racking systems without solar tracker (either with fixed tilt or allowing daily/monthly updates) is developed, which allows us to compare those systems to the ones with solar tracker (be it dual-axis tracker, polar axis racker, single-axis tracker aligned with North-South or East-West axis), taking into account both the geographical and the meteorological conditions of the sites.

The proposed methodology requires, apart from the latitude and altitude of the site, just the knowledge of the 12 values of daily averages of monthly solar irradiation (beam and diffuse). We validate it for systems with daily update by comparing our results to the values obtained using Duffie's formula with daily update, and find our values within an acceptable range (deviations of less than 2.5% in annual energy production). For systems with constant tilt, we compare method our results with Jacobson's (14), and find a very good agreement (deviations less than 0.35%).

Specifically, we study 39 cities which cover all the latitudes in the Northern Hemisphere and a large spectrum of longitudes. Using Mathematica©, we compute the optimum tilts angles for each day, month and year for systems without tracker. We also estimate the total solar irradiation for each of the possible tracking systems, compare them and compare their respective LCOE. In summary, our analysis yields the following conclusions:

(i) Obviously, dual-axis tracker systems are the most energy productive. However, they have also the worst LCOE (among those with tracker).
(ii) For polar-axis systems, the maximum loss of absorbed energy (for the locations studied) is 3.46% (always with respect to the dual-axis system) for latitudes less than 45° and 4.65% for $\lambda \geq 45°$. These have a good LCOE.
(iii) For North-South oriented systems, the loss of absorbed energy is at most 11.15% for places with $\lambda < 45°$ and 15.88 for $\lambda \geq 45°$. The LCOE is worse than for the polar-axis systems.
(iv) For East-West oriented systems, the loss of absorbed energy is at most 21.95% for $\lambda < 45°$ and 19.45% for $\lambda \geq 45°$. The LCOE of these systems is even worse than for North-South oriented ones.

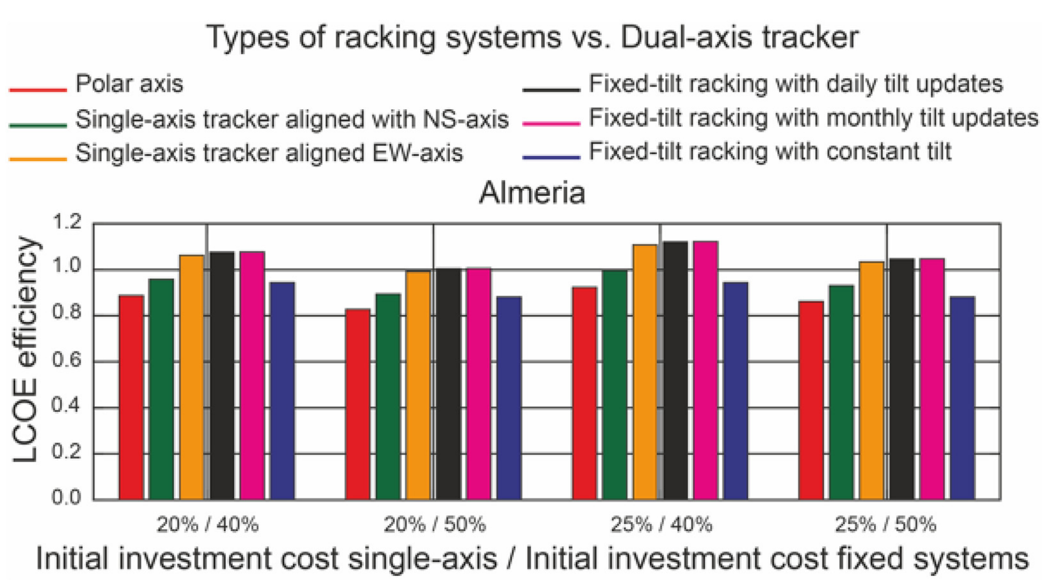

Fig. 14. Sensitivity analysis of LCOE with respect to the dual-axis tracker in Almeria.

(v) The energy loss for fixed-tilt systems with daily update with respect to East-West oriented systems is at most 3.76%.
(vi) The difference in energy absorption between fixed-tilt systems with daily update and with monthly update is negligible: this is a remarkable property which may have important budgetary consequences (both in design and maintenance costs).
(vii) In the absence of solar tracker, a system with constant tilt (no update) is consistently and significantly worse than one with monthly updates, with typical losses around 3.5% and even reaching 6.1%. However, the LCOE is much better (up to 20% better).

We consider that our methodology and its analysis can serve to make optimal decisions in the choice of racking systems of photovoltaic power systems, yielding significant benefits from the point of view of total energy absorption and budget optimization.

CRediT authorship contribution statement

A. Barbón: Conceptualization, Methodology. **P. Fortuny Ayuso:** Software, Methodology, Writing – original draft, preparation. **L. Bayón:** Conceptualization, Methodology. **C.A. Silva:** Methodology, Data curation.

Declaration of competing interest

The authors declare that they have no known competing financial interests or personal relationships that could have appeared to influence the work reported in this paper.

Acknowledgments

We wish to thank Gonvarri Solar Steel [8] for his contribution in this paper.

References

[1] BP,Statistical, Review of World Energy, 68th edition, 2019. Available from, https://www.bp.com/content/dam/bp/business-sites/en/global/corporate/pdfs/energy-economics/statistical-review/bp-stats-review-2019-full-report.pdf. (Accessed 23 December 2020). accessed on.
[2] G. Liu, M.G. Rasul, M.T.O. Amanullah, M.M.K. Khan, Techno-economic simulation and optimization of residential grid-connected PV system for the Queensland climate, Renew. Energy 45 (2012) 146–155.
[3] S. Yilmaz, H.R. Ozcalik, S. Kesler, F. Dincer, B. Yelmen, The analysis of different PV power systems for the determination of optimal PV panels and system installation—a casestudy in Kahramanmaras,Turkey, Renew. Sustain. Energy Rev. 52 (2015) 1015–1024.
[4] IEA, Trends in Photovoltaic Applications, International Renewable Energy Agency, 2019. Available from: https://www.comitesolar.cl/wp-content/uploads/2019/12/Iea-pvps_report _2019.pdf. (Accessed 23 December 2020). accessed on.
[5] IRENA, Future of solar photovoltaic: deployment, investment, technology, grid integration and socio-economic aspects, International Renewable Energy Agency, 2019. Available from: https://irena.org/-/media/Files/IRENA/Agency/Publication/2019/Nov/IRENA _Future_of_Solar_PV_2019.pdf. (Accessed 23 December 2020). accessed on.
[6] O. Savu, Good Practice: Photovoltaic Park Ciurbesti - Miroslava, European Union, [https://www.interregeurope.eu/policylearning/good-practices/item/886/photovoltaic-park-ciurbesti-miroslava-com/], accessed on 23 December 2020.
[7] R. Srivastava, A.N. Tiwari, V.K. Giri, An overview on performance of PV plants commissioned at different places in the world, Energy for Sustainable Development 54 (2020) 51–59.
[8] Gonvarri solar Steel. https://www.gsolarsteel.com/. (Accessed 23 December 2020) accessed on.
[9] Kiewit. https://www.kiewit.com/plant-insider/current-issue/fixed-tilt-vs-axis-tracker-solar-panels/. (Accessed 23 December 2020) accessed on.
[10] D.L. Talavera, Emilio Muñoz-Cerón, J.P. Ferrer-Rodríguez, P.J. Pérez-Higueras, Assessment of cost-competitiveness and profitability of fixed and tracking photovoltaic systems: the case of five specific sites, Renew. Energy 134 (2019) 902–913.
[11] NREL, Best Practices for Operation and Maintenance of Photovoltaic and Energy Storage Systems, third ed., National Renewable Energy Laboratory, Golden, CO, 2018. https://www.nrel.gov/docs/fy19osti/73822.pdf. (Accessed 23 December 2020). Accessed.
[12] J.A. Duffie, W.A. Beckman, Solar Engineering of Thermal Processes, 4 ed., John Wiley & Sons, New York, 2013.
[13] A.Z. Hafez, A. Soliman, K.A. El-Metwally, I.M. Ismail, Tilt and azimuth angles in solar energy applications – a review, Renew. Sustain. Energy Rev. 77 (2017) 147–168.
[14] N. Bailek, K. Bouchouicha, N. Aoun, M. EL-Shimy, B. Jamil, A. Mostafaeipour, Optimized fixed tilt for incident solar energy maximization on flat surfaces located in the Algerian Big South, Sustain.Energy Technol.Assessments 28 (2018) 96–102.
[15] M. Jiménez-Torres, C. Rus-Casas, L. Lemus-Zúñiga, L. Hontoria, The importance of accurate solar data for designing solar photovoltaic systems—case studies in Spain, Sustainability 9 (2017) 247–259.
[16] H. Darhmaoui, D. Lahjouji, Latitude based model for tilt angle optimization for solar collectors in the Mediterranean region, Energy Procedia 42 (2013) 426–435.
[17] M.A. Danandeh, S.M. Mousavi, Solar irradiance estimation models and optimum tilt angle approaches: a comparative study, Renew. Sustain. Energy Rev. 92 (2018) 319–330.
[18] RENEWIT, RenewIT project, Available from, http://www.renewit-project.eu/RenewIT tool: Advanced concepts and tools for renewable energy supply of IT Data Centres/, 2016. (Accessed 23 December 2020). accessed on.
[19] A. Luque, S. Hegedus, Handbook of Photovoltaic Science and Engineering, 1 ed., John Wiley & Sons, Chichester, 2003.
[20] T.P. Chang, The Sun's apparent position and the optimal tilt angle of a solar collector in the northern hemisphere, Sol. Energy 83 (2009) 1274–1284.
[21] P. Talebizadeh, M.A. Mehrabian, M. Abdolzadeh, Determination of optimum slope angles of solar collectors based on new correlations, Energy Sources Part A 33 (2011) 1567–1580.
[22] M.Z. Jacobson, V. Jadhav, World estimates of PV optimal tilt angles and ratios of sunlight incident upon tilted and tracked PV panels relative to horizontal panels, Sol. Energy 169 (2018) 55–66.
[23] A. Barbón, C. Bayón-Cueli, L. Bayón, C. Rodríguez-Suanzes, Analysis of the Tilt and Azimuth Angles of Photovoltaic Systems in Non-ideal Positions for Urban Applications, Applied Energy, 2021 in press.
[24] A. Ullah, H. Imran, Z. Maqsood, N.Z. Butt, Investigation of optimal tilt angles and effects of soiling on PV energy production in Pakistan, Renew. Energy 139 (2019) 830–843.
[25] NREL, National, solar radiation data base, Available from, http://rredc.nrel.gov/solar/old_data/nsrdb/, 2014. (Accessed 23 December 2020). accessed on.
[26] ESMAP, Solar radiation measurement data, Available from, https://energydata.info/dataset/pakistan-solar-measurement-wbg-esmap/resource/3d0dd820-b2c3-4946-a032-c7a2a4c2bd7b, 2016. (Accessed 23 December 2020). accessed on.
[27] Y. Lv, P. Si, X. Rong, J. Yan, Y. Feng, X. Zhu, Determination of optimum tilt angle and orientation for solar collectors based on effective solar heat collection, Appl. Energy 219 (2018) 11–19.
[28] CDCCMA, Climatic data center of China meteorological administration, Tsinghua University, in: Meteorological Data Set for China Building Thermal Environment Analysis (In Chinese), first ed., China Architecture & Building Press, Beijing, 2005.
[29] F. Jafarkazemi, S.A. Saadabadi, Optimum tilt angle and orientation of solar surfaces in Abu Dhabi, UAE, Renew. Energy 56 (2013) 44–49.
[30] M.D. Islam, I. Kubo, M. Ohadi, A.A. Alili, Measurement of solar energy radiation in Abu Dhabi, UAE, Renew. Energy 86 (2009) 511–515.
[31] K. Skeiker, Optimum tilt angle and orientation for solar collectors in Syria, Energy Convers. Manag. 50 (2009) 2439–2448.
[32] A.E.S.A. Nafeh, Evaluation of the optimum tilts of a PV array using maximum global insolation technique, Int. J. Numer. Model. Electron. Network. Dev. Field. 17 (2004) 385–395.
[33] N. Nijegorodov, K.R.S. Devan, P.K. Jain, S. Carlsson, Atmospheric transmittance models and an analytical method to predict the optimum slope on an absorber plate, variously orientated at any latitude, Renew. Energy 4 (1994) 529–543.
[34] H. Gunerhan, A. Hepbasli, Determination of the optimum tilt angle of solar collectors for building applications, Build. Environ. 42 (2007) 779–783.
[35] UN, World population prospects 2019, United Nations. Available from: https://population.un.org/wpp/, 2019. (Accessed 23 December 2020). accessed on.
[36] A. Barbón, P. Fortuny Ayuso, L. Bayón, J.A. Fernández-Rubiera, Predicting beam and diffuse horizontal irradiance using Fourier expansions, Renew. Energy 154 (2020) 46–57.
[37] ASHRAE Handbook, HVAC Applications. Chapter 32, ASHRAE, Atlanta (GA), 1999.
[38] C. Vernay, S. Pitaval, P. Blanc, Review of satellite-based surface solar irradiation databases for the engineering, the financing and the operating of photovoltaic systems, Energy Procedia 57 (2014) 1383–1391.
[39] A. Angström, Solar and terrestrial radiation, Q. J. Roy. Meteorol. Soc. 50 (1924) 121–125.
[40] M. Paulescu, L. Fara, E. Tulcan-Paulescu, Models for obtaining daily global solar irradiation from air temperature data, Atmos. Res. 79 (2006) 227–240.
[41] H.C. Hottel, A simple model for estimating the transmittance of direct solar

radiation through clear atmosphere, Sol. Energy 18 (1976) 129–134.
[42] B.Y.H. Liu, R.C. Jordan, The interrelationship and characteristic distribution of direct, diffuse and total solar radiation, Sol. Energy 4 (1960) 1–19.
[43] WRDC, World radiation data Centre, Available on line at, http://wrdc.mgo.rssi.ru/, 2020.
[44] D.S. Moore, W.I. Notz, M.A. Flinger, The Basic Practice of Statistics, sixth ed., W. H. Freeman, New York, 2013.
[45] B.Y.H. Liu, R.C. Jordan, The long-term average performance of flat-plate solar energy collectors, Sol. Energy 7 (1963) 53–74.
[46] T. Muneer, Solar Radiation and Day Light Models, 1 ed, Elsevier, Oxford, 2004.
[47] K.N. Shukla, S. Rangnekar, K. Sudhakar, Comparative study of isotropic and anisotropic sky models to estimate solar radiation incident on tilted surface: a case study for Bhopal, India, Energy Rep. 1 (2015) 96–103.
[48] P.S. Koronakis, On the choice of angle of tilt for south facing solar collectors in Athens Basin Area, Sol. Energy 36 (1986) 217–225.
[49] V. Badescu, 3D isotropic approximation for solar diffuse irradiance on tilted surfaces, Renew. Energy 26 (2002) 221–233.
[50] Y.Q. Tian, R.J. Davies-Colley, P. Gong, B.W. Thorrold, Estimating solar radiation on slopes of arbitrary aspect, Agric. For. Meteorol. 109 (2001) 67–74.
[51] J.W. Bugler, The determination of hourly insolation on an inclined plane using a diffuse irradiance model based on hourly measured global horizontal insolation, Sol. Energy 19 (1977) 477–491.
[52] C.C.Y. Ma, M. Iqbal, Statistical comparison of models for estimating solar radiation on inclined surgaces, Sol. Energy 31 (1983) 313–317.
[53] M. Iqbal, An Introduction to Solar Radiation, 1 ed, Academic Press Inc., New York, 1983.
[54] R. Perez, R. Seals, P. Ineichen, R. Stewart, D. Menicucci, A new simplified version of the Perez diffuse irradiance model for tited surfaces, Sol. Energy 39 (3) (1987) 221–231.
[55] R. Perez, R. Seals, J. Michalsky, All weather model for sky luminance distribution - preliminary configuration and validation, Sol. Energy 50 (3) (1993) 235–245.
[56] R.C. Temps, K.L. Coulson, Solar radiation incident upon slopes of different orientations, Sol. Energy 19 (1977) 179–184.
[57] T.M. Klucher, Evaluation of models to predict insolation on tilted surfaces, Sol. Energy 23 (1979) 111–114.
[58] D.T. Reindl, W.A. Beckman, J.A. Duffie, Diffuse fraction correlations, Sol. Energy 45 (1990) 1–7.
[59] E.D. Mehleri, P.L. Zervas, H. Sarimveis, J.A. Palyvos, N.C. Markatos, Determination of the optimal tilt angle and orientation for solar photovoltaic arrays, Renew. Energy 35 (2010) 2468–2475.
[60] J.I. Jiménez, Y. Castro-Díez, National Assembly of Geophysics and Geodesy II, 1986, p. 805.
[61] C.K. Pandey, A.K. Katiyar AK, Hourly solar radiation on inclined surfaces, Sustain.Energy Technol.Assessments 6 (2014) 86–92.
[62] G. Fubini, Opere Scelte, Edizioni Cremonese Roma, vol. 2, Unione Matematica Italiana/CNR, 1958, pp. 243–249.
[63] J. Müller, D. Folini, M. Wild, S. Pfenninger, CMIP-5 models project photovoltaics are a no-regrets investment in Europe irrespective of climate change, Energy 171 (2019) 135–148.
[64] H.Z. Al Garni, A. Awasthi, D. Wright, Optimal orientation angles for maximizing energy yield for solar PV in Saudi Arabia, Renew. Energy 133 (2019) 538–550.
[65] J. Ascencio-Vásquez, K. Brecl, M. Topič, Methodology of Köppen-Geiger-Photovoltaic climate classification and implications to worldwide mapping of PV system performance, Sol. Energy 191 (2019) 672–685.
[66] T. Tröndle, S. Pfenninger, J. Lilliestam, Home-made or imported: on the possibility for renewable electricity autarky on all scales in Europe, Energy Strategy Reviews 26 (2019) 100388.
[67] K. Branker, M.J.M. Pathak, J.M. Pearce, A review of solar photovoltaic levelized cost of electricity, Renew. Sustain. Energy Rev. 15 (2011) 4470–4482.
[68] J. Mortensen, Factors Associated with Photovoltaic System Costs, National REnewable Energy Laboratory, Golden CO, 2001.
[69] PVGIS, Joint research centre (JRC), Available from, http://re.jrc.ec.europa.eu/pvg_tools/en/tools.html#PVP, 2019. (Accessed 23 December 2020). accessed on.

Nomenclature

d: Annual degradation rate (dimensionless)
C_i: Net cost of the project (USD)
E_i: Total electrical energy output (kWh)
H_t: Total irradiation on a tilted surface (Wh/m^2)
H_t^{β}: Annual total irradiation for fixed tilt (Wh/m^2)
H_t^{n}: Annual total irradiation for fixed day (Wh/m^2)
$H_t^{\beta,m}$: Annual total irradiation for fixed tilt on each month (Wh/m^2)
I: Lifetime of the project (*years*)
I_{bh}: Beam irradiance on a horizontal surface (W/m^2)
I_{dh}: Diffuse irradiance on a horizontal surface (W/m^2)
LCOE: Levelized cost of the produced electrical energy (USD/kWh)
I_t: Total irradiance on a tilted surface (W/m^2)
n: Ordinal of the day (*day*)
r: Discount rate (dimensionless)
S_i: Availability of solar resource (Wh/m^2)
T: Solar time (h)
T_R: Sunrise solar time (h)
T_S: Sunset solar time (h)
α_S: Height angle of the Sun (rad)
β: Tilt angle of photovoltaic panel (rad)
β_{opt}^{y}: Optimal annual tilt angle (rad)
β_{opt}^{d}: Optimal daily tilt angle (rad)
β_{opt}^{m}: Optimal monthly tilt angle (rad)
γ_S: Azimuth of the Sun (rad)
δ: Solar declination (rad)
η: Performance factor of PV module (dimensionless)
η_{LCOE}: Levelized cost of the produced electrical energy efficiency (dimensionless)
θ_i: Incidence angle (rad)
θ_z: Zenith angle of the Sun (rad)
λ: Latitude angle (rad)
ω: Hour angle (rad)
ω_S: Sunset hour angle (rad)
ω_S^T: Sunset hour angle (h)